Rapid Communications

Berry curvature tomography and realization of topological Haldane model in driven three-terminal Josephson junctions

Lucila Peralta Gavensky,[1,2] Gonzalo Usaj,[1,2] D. Feinberg,[3,4] and C. A. Balseiro[1,2]

[1]*Centro Atómico Bariloche and Instituto Balseiro, Comisión Nacional de Energía Atómica, 8400 Bariloche, Argentina*

[2]*Consejo Nacional de Investigaciones Científicas y Técnicas (CONICET), Argentina*

[3]*Centre National de la Recherche Scientifique, Institut NEEL, F-38042 Grenoble Cedex 9, France*

[4]*Université Grenoble-Alpes, Institut NEEL, F-38042 Grenoble Cedex 9, France*

(Received 18 April 2018; published 25 June 2018)

We propose a protocol to locally detect the Berry curvature of the ground state of a three-terminal Josephson junction with a quantum dot based on a synchronic detection of the currents flowing into the reservoir leads when an ac modulation is applied in the device. This local gauge invariant quantity is expressed in terms of the instantaneous Green's function of the Bogoliubov–de Gennes Hamiltonian, and thus correctly accounts for the topological contribution from both the quasiparticle continuum and the Andreev bound states of the junction. We analyze the contribution to the Berry curvature from the latter by introducing an effective low-energy model. In addition, we propose to induce topological properties in the system by breaking time-reversal symmetry with a microwave field in the large frequency nonresonant regime. In the last case, the Floquet-Andreev levels are the ones that determine the topological structure of the junction, which is formally equivalent to a two-dimensional honeycomb Haldane lattice and provides a realization of this celebrated model in a solid state device. A relation between the Floquet Berry curvature and the transconductance of the driven system is derived.

DOI: 10.1103/PhysRevB.97.220505

Introduction. Multiply connected electronic networks threaded by flux tubes have been proposed several years ago as a platform to develop quantized adiabatic transport properties intimately related to topological invariants [1] with possible realizations in Josephson junctions [2]. More recently, band structures of Andreev bound states (ABS) in N-terminal Josephson junctions of conventional superconductors have been shown to host topological singularities for $N \geqslant 4$, such as zero-energy Weyl points, in the artificial reciprocal lattice space defined by the $(N-1)$-independent superconducting phases [3,4]. Even more, trijunctions may also realize nontrivial topology [5,6] when adding a magnetic flux through their central region and hence breaking time-reversal symmetry. The topological structure of these devices can be probed by means of transconductance measurements between two voltage-biased terminals which yield, at vanishing voltage, a quantized value proportional to the first Chern number of the ground state [2–4]. This global topological invariant involves an integral over phase space of a gauge invariant geometric magnitude, the Berry curvature. A nonzero Berry curvature manifests itself in physical effects, such as anomalous velocities, regardless of whether the Chern number is nontrivial [7,8]. In fact, providing experimental tools to reconstruct maps of the curvature has been a noteworthy work over the past few years [9–11].

Manifestations of topology in Josephson junctions of conventional superconductors are still an open case of study [12,13]. An interesting question to address is whether it is possible to induce topological properties on a three-terminal device by introducing a periodic driving in the superconducting phases. Indeed, nontrivial Berry curvatures can take place within the picture provided by the Floquet states. The purpose of this Rapid Communication is then twofold. First, we propose an experimentally suitable protocol to locally measure the Berry curvature of the ground-state wave function of the junction. In order to do so, we exploit one of the main advantages of these mesoscopic setups: the potential to control the superconductor phases so as to perform local transport measurements at each point of the artificial Brillouin zone. Second, we study the topology of Floquet-Andreev bands in the large frequency limit and provide a relation between their curvature and the transconductance of a biased and periodically driven setup. This constitutes a realization of the Haldane model in a solid state device [14], becoming an alternative to previous achievements in cold-atom systems [15].

Model Hamiltonian and synchronic measurement of the Berry curvature. We begin by studying a three-terminal Josephson junction (3TJJ) with a quantum dot bearing a single relevant level in the energy gap region of the superconductor (see Fig. 1). Its Hamiltonian, neglecting Coulomb interactions, can be written as

$$\mathcal{H}(t) = \sum_{\boldsymbol{k}\sigma\nu} \xi_{\boldsymbol{k}\nu} c^\dagger_{\boldsymbol{k}\sigma\nu} c_{\boldsymbol{k}\sigma\nu} - \Delta \sum_{\boldsymbol{k}\nu} (c^\dagger_{\boldsymbol{k}\uparrow\nu} c^\dagger_{-\boldsymbol{k}\downarrow\nu} + \text{H.c.}) + \varepsilon_d \sum_\sigma d^\dagger_\sigma d_\sigma + \sum_{\boldsymbol{k}\sigma\nu} (\gamma_\nu e^{-i\varphi_\nu(t)/2} d^\dagger_\sigma c_{\boldsymbol{k}\nu\sigma} + \text{H.c.}), \tag{1}$$

where we defined $\xi_{\boldsymbol{k}\nu} = \varepsilon_{\boldsymbol{k}\nu} - \mu$ and the superconducting phases have been gauged to the tunneling matrix elements between the leads and the dot. Due to gauge invariance, one of the phases is chosen to be zero without loss of generality. Even though the band structure of the ABS in equilibrium remains

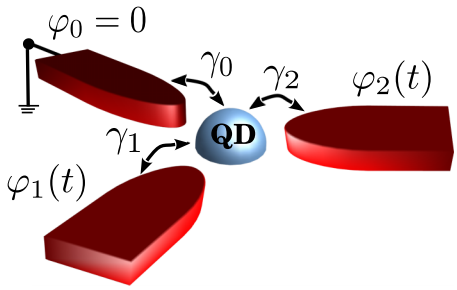

FIG. 1. General scheme of a three-terminal Josephson junction with a quantum dot. Two of the superconducting phases are changed in time by voltage biasing the leads or varying the external flux in a ring setup.

topologically trivial, its Berry curvature, defined in the (φ_1,φ_2) plane, is nonzero, provided $\varepsilon_d \neq 0$ due to breaking of particle-hole symmetry. Our first approach is to study the transport properties of the junction when making adiabatic variations of the fluxes threading the nanostructure. To this end, we use the Keldysh formalism [16,17] working in Nambu space, where the spinors in the leads and the dot are defined as $\Psi^\dagger_{\boldsymbol{k}\nu}(t) = [c^\dagger_{\boldsymbol{k}\nu\uparrow}(t), c_{-\boldsymbol{k}\nu\downarrow}(t)]$ and $\Psi^\dagger_d(t) = [d^\dagger_\uparrow(t), d_\downarrow(t)]$, respectively. The current flowing into the reservoir lead ν can be expressed as

$$\langle\phi_0|\mathcal{J}_\nu(t)|\phi_0\rangle = \frac{2e}{\hbar}\mathrm{Re}\,\mathrm{Tr}[\sigma_z \hat{V}_{\nu d}(t)\hat{\mathcal{G}}^<_{d\nu}(t,t)], \tag{2}$$

where the trace is performed in Nambu space, $[\mathcal{G}^<_{d\nu}]^{\alpha\beta}(t,t') = i\langle\phi_0|\Psi^{\dagger\beta}_\nu(t')\Psi^\alpha_d(t)|\phi_0\rangle$ are the components of the minor Green's function at the link between the dot and lead ν, and the time-dependent tunneling is given by $\hat{V}_{\nu d} = \gamma_\nu e^{i\frac{\varphi_\nu(t)}{2}}(\mathcal{I}+\sigma_z)/2 - \gamma_\nu e^{-i\frac{\varphi_\nu(t)}{2}}(\mathcal{I}-\sigma_z)/2$. In order to perform an adiabatic expansion, we will work in the Wigner representation of the two-time Green's functions, $\tilde{\mathcal{G}}(\omega,t_{\mathrm{av}}) = \int_{-\infty}^{\infty} dt_{\mathrm{rel}} e^{i\omega t_{\mathrm{rel}}}\hat{\mathcal{G}}(t,t')$, where we introduced the relative time $t_{\mathrm{rel}} = t - t'$ and the average one $t_{\mathrm{av}} = (t+t')/2$. Time derivatives of the latter are used as a small parameter, making feasible a perturbation scheme [18]. The corrections up to first order of the current expectation value are found to be [19]

$$\begin{aligned}\langle\mathcal{J}_\nu(t)\rangle &= 2e\lim_{t'-t\to\epsilon^+}\left\{-\frac{i}{\hbar}\int\frac{d\omega}{2\pi}\mathrm{Tr}\left[\frac{\partial\mathcal{H}}{\partial\varphi_\nu}\tilde{\mathcal{G}}^c_0\right] - \sum_\rho\int\frac{d\omega}{4\pi}\mathrm{Tr}\left[\epsilon^{\nu\rho}\tilde{\mathcal{G}}_0^{c^{-1}}\frac{\partial\tilde{\mathcal{G}}^c_0}{\partial\varphi_\nu}\cdot\tilde{\mathcal{G}}_0^{c^{-1}}\frac{\partial\tilde{\mathcal{G}}^c_0}{\partial\varphi_\rho}\cdot\tilde{\mathcal{G}}_0^{c^{-1}}\frac{\partial\tilde{\mathcal{G}}^c_0}{\partial\omega}\right]\dot{\varphi}_\rho\right\}\\ &= \frac{2e}{\hbar}\frac{\partial\varepsilon_g(t)}{\partial\varphi_\nu} - 2e\sum_\rho\mathcal{F}^g_{\nu\rho}(t)\dot{\varphi}_\rho(t),\end{aligned} \tag{3}$$

where $\tilde{\mathcal{G}}^c_0(\omega,t_{\mathrm{av}}) = [\omega - \mathcal{H}(t_{\mathrm{av}})]^{-1}$ is to be understood as the causal Green's function of the Hamiltonian defined in Eq. (1) in the total adiabatic limit, that is to say, the propagator that follows the perturbation instantaneously. In the last equality we made the identification of the zeroth-order mean value of the current with the phase derivative of the instantaneous ground-state energy, along with the representation of the Berry curvature of the ground state $\mathcal{F}^g_{\nu\rho}$ in terms of the single-particle time-ordered Green's function of the problem [20–22]. We therefore recover the results discussed in Ref. [3] with the virtue of identifying a way of obtaining adiabatic corrections, taking into account the continuum states to the full extent, without the need of working with the ground-state wave function.

The synchronic detection protocol to measure the Berry curvature is based on performing a periodic modulation in one of the fluxes that fixes the superconductors phase difference while keeping the other one constant. We take, without loss of generality, $\varphi_1 = \varphi^0_1$ and $\varphi_2(t) = \varphi^0_2 + b\sin(\mathcal{V}t)$. Assuming the amplitude of the driving field to be small $b \ll 1$ and the adiabatic postulate to hold, the current in lead $\nu = 1$ takes the form

$$\begin{aligned}\langle\mathcal{J}_1(t)\rangle \simeq\ & \frac{2e}{\hbar}\left(\frac{\partial\varepsilon_g}{\partial\varphi_1} + \frac{\partial^2\varepsilon_g}{\partial\varphi_2\partial\varphi_1}b\sin(\mathcal{V}t)\right)\Big|_{\boldsymbol{\varphi}^0}\\ & - 2e\mathcal{F}^g_{12}\big|_{\boldsymbol{\varphi}^0} b\,\mathcal{V}\cos(\mathcal{V}t),\end{aligned} \tag{4}$$

where we neglected terms of $\mathcal{O}(b^2)$. Hence, the zeroth- and first-order corrections are in quadrature with each other. A synchronic filter of the current flowing into the reservoir lead with the derivative of the signal can be performed, leading to a local measurement of the Berry curvature, since

$$\frac{\mathcal{V}}{2\pi}\int_0^{\frac{2\pi}{\mathcal{V}}}\langle\hat{J}_1(t)\rangle\cos(\mathcal{V}t)dt = -e\mathcal{F}^g_{12}|_{\boldsymbol{\varphi}^0} b\mathcal{V}. \tag{5}$$

In order to compare the full numerical results with a simpler model, we introduce a low-energy approximation of the ABS [23–25], with an effective Hamiltonian given by

$$\hat{H}_{\mathrm{eff}}(\boldsymbol{\varphi}) = -\hat{G}^{-1}_{dd}(\omega=0) = \begin{pmatrix}\varepsilon_d & \sum_\nu\Gamma_\nu e^{-i\varphi_\nu}\\ \sum_\nu\Gamma_\nu e^{i\varphi_\nu} & -\varepsilon_d\end{pmatrix}, \tag{6}$$

where the anomalous on-site interaction is expressed in terms of the hybridization $\Gamma_\nu = -\gamma^2_\nu\rho(\varepsilon_F)\pi$. This limit is expected to be generally accurate whenever $\gamma_\nu \ll \Delta$, so that the bound states possess a weak hybridization with the continuum above the gap. It is then possible to define an effective Berry curvature given by

$$\mathcal{F}^{\mathrm{eff}}_{21}(\boldsymbol{\varphi}) = \frac{1}{2\pi}\hat{\boldsymbol{h}}_{\mathrm{eff}}\cdot(\partial_{\varphi_2}\hat{\boldsymbol{h}}_{\mathrm{eff}}\times\partial_{\varphi_1}\hat{\boldsymbol{h}}_{\mathrm{eff}}), \tag{7}$$

with $\boldsymbol{h}_{\mathrm{eff}} = [\Gamma_0 + \Gamma_1\cos(\varphi_1) + \Gamma_2\cos(\varphi_2), \Gamma_1\sin(\varphi_1) + \Gamma_2\sin(\varphi_2), \varepsilon_d]$ and $\hat{\boldsymbol{h}}_{\mathrm{eff}} = \boldsymbol{h}_{\mathrm{eff}}/|\boldsymbol{h}_{\mathrm{eff}}|$.

Interestingly, the Hamiltonian in Eq. (6) enjoys all the topological information of a honeycomb lattice in a tight-binding description, identifying $\varphi_\nu = \boldsymbol{k}\cdot\boldsymbol{a}_\nu$ with $\boldsymbol{a}_\nu$ the displacements of a site respect to its three nearest neighbors and $2\varepsilon_d$ the subblatice energy difference. In what follows, we perform an

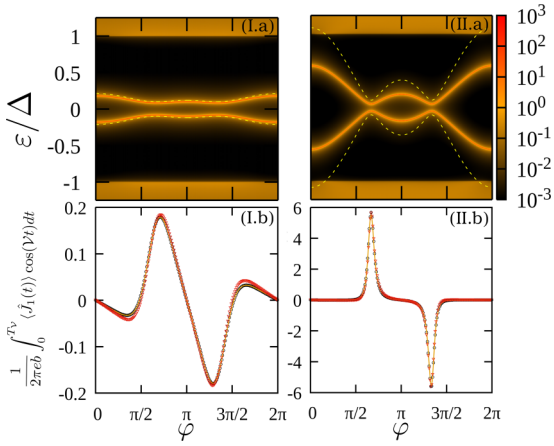

FIG. 2. Upper panels show the dot spectral density in units of Δ along $\varphi = \varphi_1 = -\varphi_2$ for a symmetric 3TJJ in equilibrium with a hopping amplitude to the leads (I.a) $\gamma = 0.25\Delta$ and (II.a) $\gamma = 0.6\Delta$. The dot energy was taken to be $\varepsilon_d = 0.1\Delta$ in both cases. Dashed lines indicate the dispersion of Andreev levels captured by the infinite-gap limit. Lower panels (I.b) and (II.b) show the corresponding outcome of the filter of the $\cos(\mathcal{V}t)$ component of the current flowing into the biased lead $\nu = 1$ obtained using Keldysh formalism (open circles) and its comparison with both the Berry curvature of the exact Hamiltonian $\mathcal{F}^g_{21}$ [Eq. (3)] (solid line) and the one obtained with Eq. (7) (triangles).

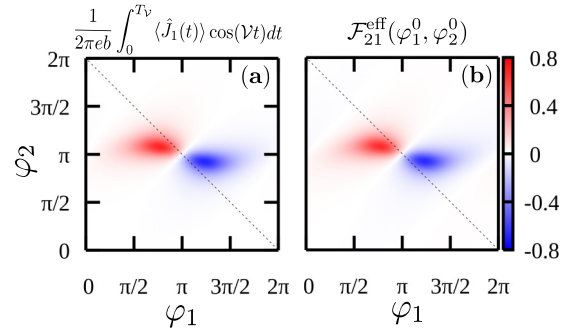

FIG. 3. (a) Synchronic filter of the of the current flowing into the biased lead $\nu = 1$ as obtained from Eq. (5) using Keldysh formalism throughout the whole phase space. (b) Berry curvature obtained within the low-energy effective Hamiltonian describing the infinite-gap limit.

exact calculation of the current as expressed in Eq. (2) taking into account the perturbation to all orders by making use of the time periodicity of the Green's functions [19] and compare its synchronic filter with the Berry curvature. In Fig. 2 results for a symmetric 3TJJ ($\gamma_\nu = \gamma$) are shown. The dot spectral density $A_d(\omega) = -(1/\pi)\mathrm{Im}\,\mathrm{Tr}(G^r_{dd})$ is depicted for different values of γ/Δ along the high-symmetry path $\varphi_1 = -\varphi_2$, finding a good agreement with the bands of $\hat{H}_{\mathrm{eff}}$ (indicated with dashed lines) for $\gamma = 0.25\Delta$ [Fig. 2(I.a)]. As expected, this description turns out to be insufficient for $\gamma = 0.6\Delta$ [Fig. 2(II.a)]. In both cases the dot energy is $\varepsilon_d = 0.1\Delta$. The lower panels (I.b) and (II.b) show the corresponding filter of the current flowing into the reservoir lead $\nu = 1$ as obtained from Eq. (5) and its comparison with both $\mathcal{F}^g_{21}$ [see Eq. (3)] and the low-energy approximation of this quantity given by the effective model $\mathcal{F}^{\mathrm{eff}}_{21}$ [Eq. (7)]. In the spirit of the adiabatic approximation to be valid, the frequency was chosen to be $\mathcal{V} = 10^{-2}\Delta$ and the field amplitude $b = 10^{-4}\Delta$. We observe that the synchronic protocol gives a precise information on the curvature of the Andreev bands captured by the low-energy theory even when the hybridization with the states above the superconductor gap is relevant. We can comprehend this behavior by noticing that the Berry curvature in this model is a low-energy localized quantity. In both cases, even though the integral over the whole phase space of the Berry curvature is zero, the current has a topological Thouless contribution whenever the phases of the junction are near the Dirac points.

This procedure can be done along the whole phase space, so as to obtain a map of the Berry curvature with the proposed transport measurement. In Fig. 3 we show the comparison for an asymmetric junction with hoppings $\gamma_1 = 0.3\Delta$, $\gamma_2 = 0.5\Delta$, and $\gamma_3 = 0.6\Delta$ of the low-energy model with the results of the finite-gap Hamiltonian using the Keldysh formalism. We find an excellent agreement between both, which guarantees the validity of the approximation given by Eq. (6). We thus conclude that the effect of the continuum states on the topological properties of this model is negligible. It is worth emphasizing, however, that our expression for the transconductance [second term in Eq. (3)] reproduces the correct quantized average value [26] even when the continuum does contribute as in the model presented in Ref. [5].

Inducing topology by driving. Floquet-Andreev physics. When introducing a periodic driving that breaks time-reversal symmetry (TRS) into the three-terminal junction, the resulting Floquet system can have topological properties which differ from the original one. This can be engineered by introducing an "elliptically" polarized driving of the form $\delta\varphi_\nu(t) = A_0\cos(\Omega t + \chi_\nu)$ with $\chi_1 - \chi_2$ not a π-multiple [27]. The Floquet Hamiltonian of the system is given by $[\mathcal{H}_F]_{mn} = (H_0 - m\Omega)\delta_{mn} + \mathcal{U}_{m-n}$, with H_0 representing the undriven Hamiltonians of the dot and leads and $\mathcal{U}_{m-n} = 1/T\int_0^T e^{i(m-n)\Omega t}\mathcal{U}(t)$ the $(m-n)$th harmonic of the time-dependent tunneling. The Floquet Green's functions satisfy $[\omega - \mathcal{H}_F]\mathcal{G}^F(\omega) = \mathcal{I}$, and its matrix elements can be used to reconstruct the full two-time-dependent original Green's function [28]

$$\check{\mathcal{G}}(t,t') = \sum_{m,n}\int_0^\Omega \frac{d\omega}{2\pi} e^{-i(\omega+m\Omega)t} e^{i(\omega+n\Omega)t'}\mathcal{G}^F_{mn}(\omega). \quad (8)$$

In Fig. 4(a) we show the spectral density of the Floquet Green's function of the dot projected onto the zeroth replica $A^F_d = -(1/\pi)\mathrm{Im}\,\mathrm{Tr}_{00}[\mathcal{G}^F_{dd}(\omega)]$ for $\chi_1 - \chi_2 = \pi/2$, $\varepsilon_d = 0$, $\Omega = 0.4\Delta$, and $A_0 = 0.8$. In this case symmetric hoppings $\gamma_\nu = 0.25\Delta$ were chosen and a representation along the path $\varphi_2 = -\varphi_1$ is shown. The breaking of TRS removes the degeneration at the diabolical Dirac points, producing the appearance of a zero-energy gap in the Floquet spectrum. In Fig. 4(b) we show a zoom of the spectral density near the Fermi level along with a comparison with the Floquet eigenergies obtained from the effective low-energy theory, expected to remain suitable for these parameters. Indeed, since the energy of the microwave field is larger than the bandwith of the Andreev bands, the only relevant topological change can take place at zero energy, since no gaps at the first Floquet zone boundary ($\varepsilon = \pm\hbar\Omega/2$) can be present. On the other hand, the first Floquet replicas of the Andreev band structure lie within the superconductors gap so

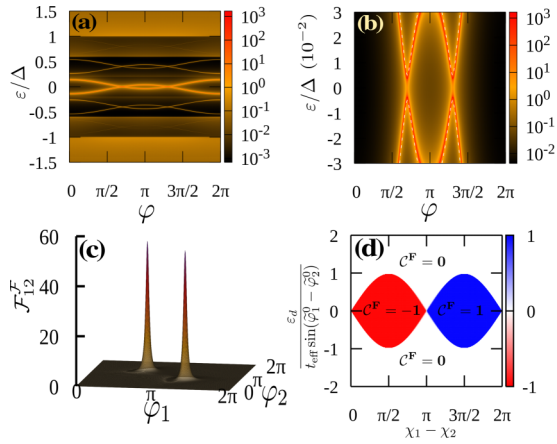

FIG. 4. (a) Spectral density of the Floquet Green's function of the dot projected onto the zeroth replica for $\Omega = 0.4\Delta$, $A_0 = 0.8$, and $\varepsilon_d = 0$. (b) Zoom of the spectral density near zero energy, where a gap opens due to breaking of TRS. Dashed lines indicate the dispersion relation of the Floquet eigenergies obtained within the *infinite-gap* approximation. (c) Berry curvature of the Floquet-Andreev band in phase space with parameters as in (a). (d) Floquet Chern numbers of the junction as a function of the polarization of the driving.

that the continuum states will renormalize only perturbatively the dispersion relation of the Floquet bands at low energy. In Fig. 4(c) the Berry curvature of the lower Floquet-Andreev band obtained with the driven effective model is shown. In this case, both Dirac points contribute with the same topological charge leading to a nontrivial Chern number. Standard Brillouin-Wigner perturbation theory in $1/\Omega$ yields, in this regime, a Haldane-like effective Floquet Hamiltonian on the projected zero photon subspace [29,30], with renormalized parameters of the form

$$\widetilde{\varepsilon}_d(\boldsymbol{\varphi}^{\mathbf{0}}) = \varepsilon_d - t_{\rm eff}\sin\left(\varphi_1^0 - \varphi_2^0\right)\sin(\chi_1-\chi_2),$$
$$\widetilde{\Gamma}_{1(2)} = \Gamma_{1(2)}J_0(A_0), \tag{9}$$

and $t_{\rm eff} = 4\Gamma_1\Gamma_2 J_1^2(A_0)/\hbar\Omega$ acting as a second-neighbor effective hopping in the previously mentioned honeycomb lattice description. The Dirac points in the symmetric model ($\Gamma_\nu = \Gamma$) are displaced from their original position along the path $\widetilde{\varphi}_2^0 = -\widetilde{\varphi}_1^0$ such that $\cos(\widetilde{\varphi}_1^0) = -1/2J_0(A_0)$. The topological phase diagram of the driven trijunction is shown in Fig. 4(d) as a function of polarization, which measures the breaking of TRS. The dot energy has been normalized to the value it takes when the gap closes for "circularly" polarized driving.

A crucial issue concerns the possibility of following adiabatically the Floquet states in order to accurately probe their properties. The equilibrium populations are strongly modified whenever a gap opens in the spectrum so that the most probable scenario is that the wave function at these singular phases behaves as a superposition of Floquet states, leading to a nonthermal occupation of the Floquet bands. Nonetheless, if the phases of the superconductors are set up far away from the latter, there is a precise adiabatic connection between the unperturbed Hamiltonian and the dressed Floquet-Andreev bands. We now show that voltage biasing these adiabatically connected states can provide information on the Berry curvature of the Floquet bands. In order to do so we appeal to the two-time formalism [31–33]. Under this formulation, an extended Schrödinger equation is taken into account, $[\mathcal{H}(t,\tau) - i\hbar\partial_t]|\psi(t,\tau)\rangle\rangle = i\hbar\partial_\tau|\psi(t,\tau)\rangle\rangle$, where the time variable t is associated with the fast time-periodic evolution of frequency Ω, while τ accounts for the slow time dynamics generated by the bias voltages at the leads, i.e., the phases are such that $\varphi_\nu(t,\tau) = \theta_\nu(t) + \phi_\nu(\tau)$, with $\theta_\nu(t) = A_0\cos(\Omega t + \lambda_\nu)$ and $\phi_\nu(\tau) = \varphi_\nu^0 + \frac{2e}{\hbar}V_\nu\tau$. The notation $|\cdots\rangle\rangle$ indicates that the two-time wave functions are to be treated in a Hilbert space with the internal product $\langle\langle\psi^\alpha(\tau)|\psi^\beta(\tau)\rangle\rangle = \frac{1}{T}\int_0^T\langle\psi^\alpha(\tau,t)|\psi^\beta(\tau,t)\rangle dt$. The adiabatic basis of the problem is the Floquet basis, meaning that these are the states $|u_\beta^F(t,\tau)\rangle\rangle$ that satisfy the instantaneous Floquet equation $[\mathcal{H}(t,\tau) - i\hbar\partial_t]|u_\beta^F(t,\tau)\rangle\rangle = \varepsilon_\beta^F(\tau)|u_\beta^F(t,\tau)\rangle\rangle$, where $\beta = 1,2$ indexes the two bands of the first Floquet zone with quasienergies $-\hbar\Omega/2 < \varepsilon_\beta^F < \hbar\Omega/2$. When treating the bias as an adiabatic perturbation in the slow scale, the mean value of the current operator at each lead is found to be

$$\langle\langle\mathcal{J}_\nu\rangle\rangle_\alpha = \frac{2e}{\hbar}\frac{\partial\varepsilon_\alpha^F}{\partial\varphi_\nu}[\boldsymbol{\phi}(\tau)] - \frac{4e^2}{\hbar}\sum_\rho\mathcal{F}_{\nu\rho}^{F\alpha}[\boldsymbol{\phi}(\tau)]V_\rho, \tag{10}$$

where the first term corresponds to the adiabatic Floquet-Josephson supercurrent and the second accounts for the Berry curvature of the α-Floquet state,

$$\mathcal{F}_{\nu\rho}^{F\alpha} = i\left[\left\langle\left\langle\partial_{\varphi_\nu}u_\alpha^F|\partial_{\varphi_\rho}u_\alpha^F\right\rangle\right\rangle - \left\langle\left\langle\partial_{\varphi_\rho}u_\alpha^F|\partial_{\varphi_\nu}u_\alpha^F\right\rangle\right\rangle\right]. \tag{11}$$

We arrive at an expression for the currents with a transconductance term proportional to the gauge field, in analogy with the results obtained for undriven setups in Ref. [3]. If incommensurate voltages were to be applied, so that the entire phase space is probed after a considerable time, then Eq. (10) results in a topologically quantized transconductance since

$$\int_{\rm BZ}\frac{d^2\varphi}{(2\pi)^2}\langle\langle\mathcal{J}_\nu\rangle\rangle_\alpha = -\frac{4e^2}{h}\sum_\rho C_{\nu\rho}^{F\alpha}V_\rho, \tag{12}$$

where $C_{\nu\rho}^{F\alpha}$ is the Chern number of the Floquet band α.

Conclusion. We have proposed a protocol to perform local measurements of the Berry curvature of the ground-state wave function of Josephson junctions. This gauge invariant quantity [Eq. (3)] is obtained with the Feynman propagator of the Hamiltonian which includes the quasiparticle continuum and compared with a low-energy effective model of the ABS spectrum. We found a good agreement between both since the gauge field of the model is localized at energies close to zero. On the other hand, we have put forward a way of inducing topological properties on three-terminal devices by introducing a periodic driving that breaks time-reversal symmetry and generates dressed Floquet-Andreev bands with nontrivial Haldane-like Chern numbers. We have proposed that the transconductance of the driven junction yields information of the Floquet Berry curvature when voltage biasing states adiabatically connected to the Floquet bands.

Acknowledgments. We acknowledge financial support from PICTs 2013-1045 and 2016-0791 from ANPCyT, PIP 11220150100506 from CONICET, and Grant No. 06/C526 from SeCyT-UNC. D.F. acknowledges useful discussions with Y. V. Nazarov, J. S. Meyer, and M. Houzet.

[1] J. E. Avron, A. Raveh, and B. Zur, Adiabatic quantum transport in multiply connected systems, Rev. Mod. Phys. **60**, 873 (1988).

[2] J. E. Avron and M. C. Cross, Integer charge transport in Josephson junctions, Phys. Rev. B **39**, 756 (1989).

[3] R.-P. Riwar, M. Houzet, J. S. Meyer, and Y. V. Nazarov, Multi-terminal Josephson junctions as topological matter, Nat. Commun. **7**, 11167 (2016).

[4] E. Eriksson, R.-P. Riwar, M. Houzet, J. S. Meyer, and Y. V. Nazarov, Topological transconductance quantization in a four-terminal Josephson junction, Phys. Rev. B **95**, 075417 (2017).

[5] J. S. Meyer and M. Houzet, Nontrivial Chern Numbers in Three-Terminal Josephson Junctions, Phys. Rev. Lett. **119**, 136807 (2017).

[6] H.-Y. Xie, M. G. Vavilov, and A. Levchenko, Topological Andreev bands in three-terminal Josephson junctions, Phys. Rev. B **96**, 161406 (2017).

[7] G. Sundaram and Q. Niu, Wave-packet dynamics in slowly perturbed crystals: Gradient corrections and Berry-phase effects, Phys. Rev. B **59**, 14915 (1999).

[8] D. Xiao, M.-C. Chang, and Q. Niu, Berry phase effects on electronic properties, Rev. Mod. Phys. **82**, 1959 (2010).

[9] N. Flaschner, B. S. Rem, M. Tarnowski, D. Vogel, D.-S. Luhmann, K. Sengstock, and C. Weitenberg, Experimental reconstruction of the Berry curvature in a Floquet Bloch band, Science **352**, 1091 (2016).

[10] T. Li, L. Duca, M. Reitter, F. Grusdt, E. Demler, M. Endres, M. Schleier-Smith, I. Bloch, and U. Schneider, Bloch state tomography using Wilson lines, Science **352**, 1094 (2016).

[11] M. Wimmer, H. M. Price, I. Carusotto, and U. Peschel, Experimental measurement of the Berry curvature from anomalous transport, Nat. Phys. **13**, 545 (2017).

[12] E. Strambini, S. D'Ambrosio, F. Vischi, F. S. Bergeret, Y. V. Nazarov, and F. Giazotto, The ω-SQUIPT as a tool to phase-engineer Josephson topological materials, Nat. Nanotechnol. **11**, 1055 (2016).

[13] F. Vischi, M. Carrega, E. Strambini, S. D'Ambrosio, F. S. Bergeret, Y. V. Nazarov, and F. Giazotto, Coherent transport properties of a three-terminal hybrid superconducting interferometer, Phys. Rev. B **95**, 054504 (2017).

[14] F. D. M. Haldane, Model for a Quantum Hall Effect without Landau Levels: Condensed-Matter Realization of the "Parity Anomaly", Phys. Rev. Lett. **61**, 2015 (1988).

[15] G. Jotzu, M. Messer, R. Desbuquois, M. Lebrat, T. Uehlinger, D. Greif, and T. Esslinger, Experimental realization of the topological Haldane model with ultracold fermions, Nature (London) **515**, 237 (2014).

[16] H. Haug and A.-P. Jauho, *Quantum Kinetics in Transport and Optics of Semiconductors* (Springer, Berlin, 1996).

[17] J. C. Cuevas, A. Martín-Rodero, and A. Levy Yeyati, Hamiltonian approach to the transport properties of superconducting quantum point contacts, Phys. Rev. B **54**, 7366 (1996).

[18] V. F. Kershaw and D. S. Kosov, Nonequilibrium Green's function theory for nonadiabatic effects in quantum electron transport, J. Chem. Phys. **147**, 224109 (2017).

[19] See Supplemental Material at http://link.aps.org/supplemental/10.1103/PhysRevB.97.220505 for a detailed demonstration of the expression of the first adiabatic correction of the current expectation value in terms of the time ordered Green's functions using perturbation theory in the average time t_{av}. The Keldysh formalism and the Floquet representation of the Green's functions used to calculate the currents flowing into the reservoir leads is also discussed.

[20] Q. Niu, D. J. Thouless, and Y.-S. Wu, Quantized Hall conductance as a topological invariant, Phys. Rev. B **31**, 3372 (1985).

[21] V. Gurarie, Single-particle Green's functions and interacting topological insulators, Phys. Rev. B **83**, 085426 (2011).

[22] Z. Wang and S.-C. Zhang, Simplified Topological Invariants for Interacting Insulators, Phys. Rev. X **2**, 031008 (2012).

[23] J. Bauer, A. Oguri, and A. C. Hewson, Spectral properties of locally correlated electrons in a Bardeen-Cooper-Schrieffer superconductor, J. Phys.: Condens. Matter **19**, 486211 (2007).

[24] I. Affleck, J.-S. Caux, and A. M. Zagoskin, Andreev scattering and Josephson current in a one-dimensional electron liquid, Phys. Rev. B **62**, 1433 (2000).

[25] E. Vecino, A. Martín-Rodero, and A. Levy Yeyati, Josephson current through a correlated quantum level: Andreev states and π junction behavior, Phys. Rev. B **68**, 035105 (2003).

[26] L. Peralta Gavensky *et al.* (unpublished).

[27] B. Venitucci, D. Feinberg, R. Mélin, and B. Douçot, Nonadiabatic Josephson current pumping by chiral microwave irradiation, Phys. Rev. B **97**, 195423 (2018).

[28] N. Tsuji, T. Oka, and H. Aoki, Correlated electron systems periodically driven out of equilibrium:Floquet+DMFT formalism, Phys. Rev. B **78**, 235124 (2008).

[29] T. Kitagawa, T. Oka, A. Brataas, L. Fu, and E. Demler, Transport properties of nonequilibrium systems under the application of light: Photoinduced quantum Hall insulators without Landau levels, Phys. Rev. B **84**, 235108 (2011).

[30] T. Mikami, S. Kitamura, K. Yasuda, N. Tsuji, T. Oka, and H. Aoki, Brillouin-Wigner theory for high-frequency expansion in periodically driven systems: Application to Floquet topological insulators, Phys. Rev. B **93**, 144307 (2016).

[31] U. Peskin and N. Moiseyev, The solution of the time-dependent Schrödinger equation by the (t,t') method: Theory, computational algorithm, and applications, J. Chem. Phys. **99**, 4590 (1993).

[32] P. Pfeifer and R. D. Levine, A stationary formulation of time-dependent problems in quantum mechanics, J. Chem. Phys. **79**, 5512 (1983).

[33] K. Drese and M. Holthaus, Floquet theory for short laser pulses, Eur. Phys. J. D **5**, 119 (1999).